Effect of Different Alkali-assisted Deposition Precipitation Methods on the Durability of Three-way Catalysts

FAN Jun[1], JIANG Xue[2], JIAO Yi[2], CHEN Yusheng[1], WANG Jianli[1], CHEN Yaoqiang[1,2]

(1. College of Chemistry, Sichuan University, Chengdu 610064, China; 2. Institute of New Energy and Low-Carbon Technology, Sichuan University, Chengdu 610064, China)

Abstract: The aging treatment always brings about severe deactivation of three-way catalysts (TWCs) so that improving the durability is one goal of TWCs design. In this work, $Pt/Ce_{0.4}Zr_{0.5}La_{0.05}Pr_{0.05}O_2$ (Pt/CZ) TWCs were prepared by two different alkali-assisted deposition precipitation method, urea or ammonia. The effects of different alkali-assisted on the physicochemical properties, catalytic activity and durability were analyzed. It was found that the Pt/CZ catalyst prepared by urea-assisted deposition precipitation method (UDP) had poor aging resistance but the Pt/CZ catalyst prepared by ammonia-assisted (ADP) showed better anti-aging ability. Based on the results of XRD, CO adsorption, XPS and H_2-TPR, comparatively larger particle size of Pt species and stronger interaction for ADP make it more difficult to sinter together during the aging treatment, which is favorable for maintaining catalytic activity. Therefore, the ADP catalyst shows a bright future for industrialization.

Key words: three-way catalysts; deposition precipitation; alkali-assisted; durability

Three-way catalysts (TWCs) are one of the most important catalysts in purifying exhaust gas from gasoline powered vehicles[1-2], which are able to effectively convert hazardous carbon monoxide (CO), nitrogen oxides (NO_x), hydrocarbons (HC) to harmless carbon dioxide (CO_2), water (H_2O) and nitrogen (N_2) simultaneously[3-4]. However, aging is the main cause of catalyst deactivation due to the serious influence on the structural and textural properties, metal dispersion, oxygen storage capacity (OSC) and redox ability[5-6]. It is necessary to design TWCs with high stability to meet increasingly durability requirement[7-8]. Researchers have done a lot of work to improve the thermal stability of TWCs[9-10], suppressing phase transformation and preventing the sintering of active noble metal. No matter which strategy, the typical formulation of TWCs is unchanged because of their preferable poisoning resistance and higher thermal stability[10-11]. Generally, changing the preparation method is a simple and easy route to improve the durability of TWCs[12-13].

The deposition precipitation method is one of the main preparation methods for industrial catalysts, which is done in the presence of an existing support, and a precursor solution usually forms metal hydroxides by injection of the precipitant[14]. Thomas, et al.[15] used deposition precipitation method to prepare Co/TiO_2 catalysts using urea hydrolysis or ammonia evaporation. Moreau, et al.[16] prepared Au/TiO_2 catalyst by deposition precipitation method with NaOH as precipitant. The deposition precipitation method has been widely used in the preparation of catalysts, but it is rarely used in the preparation of noble metal TWCs. Therefore, it is valuable to study the deposition precipitation method for the preparation of TWCs.

In the present work, we have prepared ceria-zirconia-supported platinum (Pt/CZ) catalysts with different alkali-assisted deposition precipitation method, and a Pt/CZ catalyst prepared by impregnation method as reference catalyst. The effect of different alkali-assisted deposition precipitation methods on the stability of TWCs were investigated.

1 Experimental

1.1 Catalyst preparation

The metal precursor was H_2PtCl_6 (0.10 g/mL) aqueous solution and the loading content of Pt was 1wt%. The

support material, a mixed oxide of CeO_2-ZrO_2-La_2O_3-Pr_2O_5 (the mass ratio of 40/50/5/5, CZ) was supplied by Rhodia Company. The benchmark Pt/CZ was prepared by traditional impregnation method (IM). The catalyst prepared by deposition-precipitation method assisted with urea (molar ratio of urea/Pt = 50) was labeled as UDP. Another catalyst prepared by deposition-precipitation method assisted with ammonia at pH = 9 was labeled as ADP. All samples were dried in an oven at 90 ℃ for 1 d and calcined at 550 ℃ for 3 h in air. The as-prepared powders were sprinkled onto cordierite to obtain the monolithic catalyst with a loading capacity of (160±5) g/L. Afterwards the monolithic catalysts were calcined at 550 ℃ for 3 h in air to obtain the fresh catalysts. The fresh catalysts were hydrothermal treated in 10vol% H_2O/air at 750 ℃ for 13 h to obtain aged catalysts, which were labeled as IM-a, UDP-a and ADP-a, respectively.

1.2 Catalyst characterization

The textural properties of the catalysts were obtained by Quantachrome automated surface area and pore size analyzer (Autosorb SI). The powder X-ray diffraction (XRD) patterns were recorded on Philips Company (PW 1730). The dispersion of Pt species was performed on CO pulse adsorption and Fourier transform infrared spectrometer (FT-IR, Thermo Nicolet 6700). X-ray photoelectron spectroscopy (XPS) experiments were carried out on an electron spectrometer (XSAM-800). Hydrogen-temperature programmed reduction (H_2-TPR) was performed in a tubular quartz microreactor and recorded by thermal conductivity detector (TCD).

1.3 Activity tests

The catalytic performance were evaluated using a fixed-bed continuous flow reactor by passing through a simulated gasoline engine exhaust gas mixture, which was composed of CO (4600×10^{-6}), C_3H_6 (220×10^{-6}), C_3H_8 (110×10^{-6}), H_2 (1533×10^{-6}), NO (1250×10^{-6}), CO_2 (10%), H_2O (10%), O_2 (3600×10^{-6}) and N_2 (balance gas). The gas hourly space velocity (GHSV) was controlled at 5×10^4 h^{-1}.

2 Results and discussion

2.1 Textural and structural characterization

The textural parameters of the support and catalysts are listed in Table 1. It can be seen that the specific surface area and pore volume of samples are similar with each other. However, the average pore radii of UDP-a and ADP-a are smaller than that of IM-a. This may be attributed to that the Pt species are more likely to enter the small pores of support in the preparation of UDP and ADP. The presence of Pt in the small pores is conducive to maintaining the pores in the aging process[17].

The X-ray diffraction patterns and relative intensity of Pt (111) are shown in Fig. 1. It is observed from Fig. 1(a) that the diffraction peaks of all samples are characteristic of cubic CeO_2-ZrO_2 (CZ) phase[18]. There are no peaks of Pt or PtO_x in IM and UDP, which may be attributed to the good dispersion of Pt species on support. However, it is clear to find out that the diffraction peaks of Pt in ADP, confirming the existence of larger Pt particles in ADP. After aging, the peaks identified as Pt phase are observed for all samples due to the agglomeration of noble metal. The relative intensity of Pt (111) peak of these catalysts are shown in Fig. 1(b). The order of diffraction peak intensity can be recorded as UDP-a > IM-a > ADP-a. This indicates that Pt particles are the smallest in the ADP-a.

Table 1 Textural and structural parameters of the support and samples

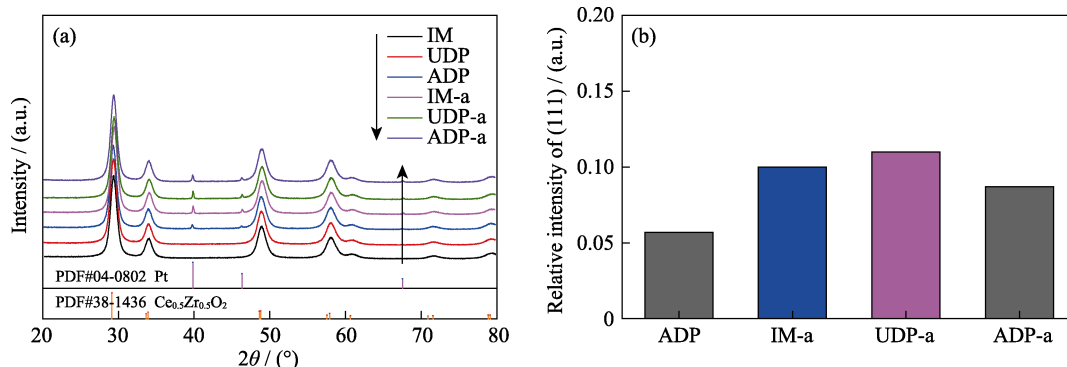| Samples	Surface area/ ($m^2 \cdot g^{-1}$)	Pore volume/ ($mL \cdot g^{-1}$)	Average pore radius/nm
IM	60	0.23	7.5
UDP	63	0.22	7.5
ADP	61	0.23	7.7
IM-a	49	0.24	9.4
UDP-a	50	0.22	7.6
ADP-a	53	0.25	7.7
CZLP	64	0.25	8.7

Fig. 1 XRD patterns of fresh and aged samples (a) and the comparison of their relative intensities of Pt (111) based on the strongest peak of support (b)

2.2   CO chemisorption results

The dispersion of Pt species was evaluated by CO pulse adsorption method, and the obtained results are depicted in Fig. 2(a). The dispersion of Pt species for fresh samples follow the order of UDP > IM > ADP which coincides with the XRD results. For the aged samples, the dispersion of Pt species sharply declines owing to the aggregation of noble metal particles.

The CO adsorption experiment was also performed on an FT-IR equipment and the obtained CO-FTIR spectrum were presented in Fig. 2(b, c). The IR band exhibited in figures are assigned to CO species linearly adsorbed on Pt^0[19]. For the fresh samples, the intensity of band decreased with an order of IM ≈ UDP > ADP, which reflects the dispersion of Pt species to some extent[20]. As for aged samples, compared with fresh samples, the band strength of UDP-a decreases more greatly, while that of ADP-a samples decreases more slightly, which indicates that ADP owns good hydrothermal stability. This is consistent with the results of XRD analysis.

2.3   XPS analysis

X-ray photoelectron spectroscopy (XPS) experiment was performed to clarify the surface elemental states of samples. The relative amounts of Ce, O and Pt are listed in Table 2, and the obtained spectra of O1s, Ce3d and Pt4f are illustrated in Fig. 3. The spectra of O1s (Fig. 3(a, d)) are composed of two characteristic peaks with the corresponding binding energy (BE) values of 529.2 and 531.2 eV. One at 529.2 eV is denoted as lattice oxygen (O$_{latt}$), and the other at 531.2 eV is attributed to surface adsorbed oxygen (O$_{ads}$)[21]. The spectra of Ce3d (Fig. 3(b, e)) are deconvoluted into eight peaks corresponding to four pairs of spin-orbit doublets. The peaks labeled as v, v'', v''' and u, u'', u''' are assigned to Ce^{4+}, and an additional doublet (v', u') are arisen from Ce^{3+} species[20]. For the XPS spectra of Pt4f (c, f), the peak at 70.7 eV is assigned to Pt^0 and that at 72.4 eV is ascribed to PtO. Moreover, the peaks locating at 74.0 eV is attributed to PtO$_2$[22].
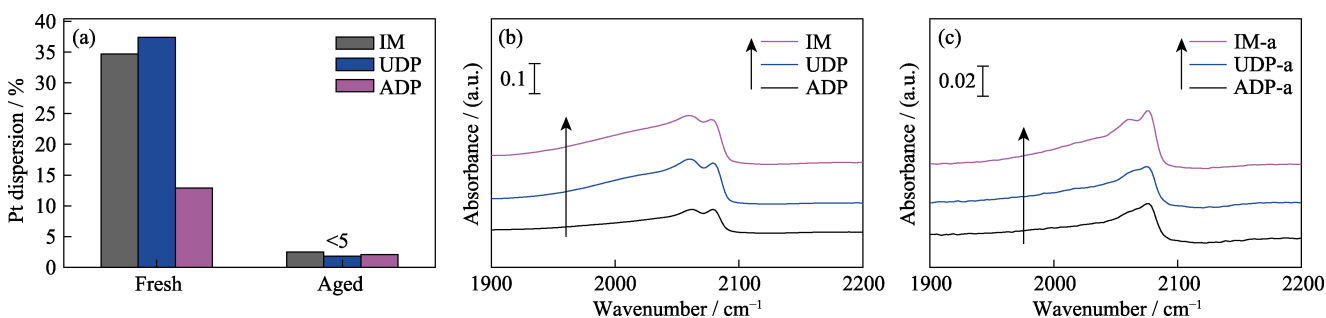

Fig. 2   Pt dispersion of samples measured by CO-chemisorption method (a) and FT-IR spectra of CO absorbed on the fresh (b) and aged (c) samples
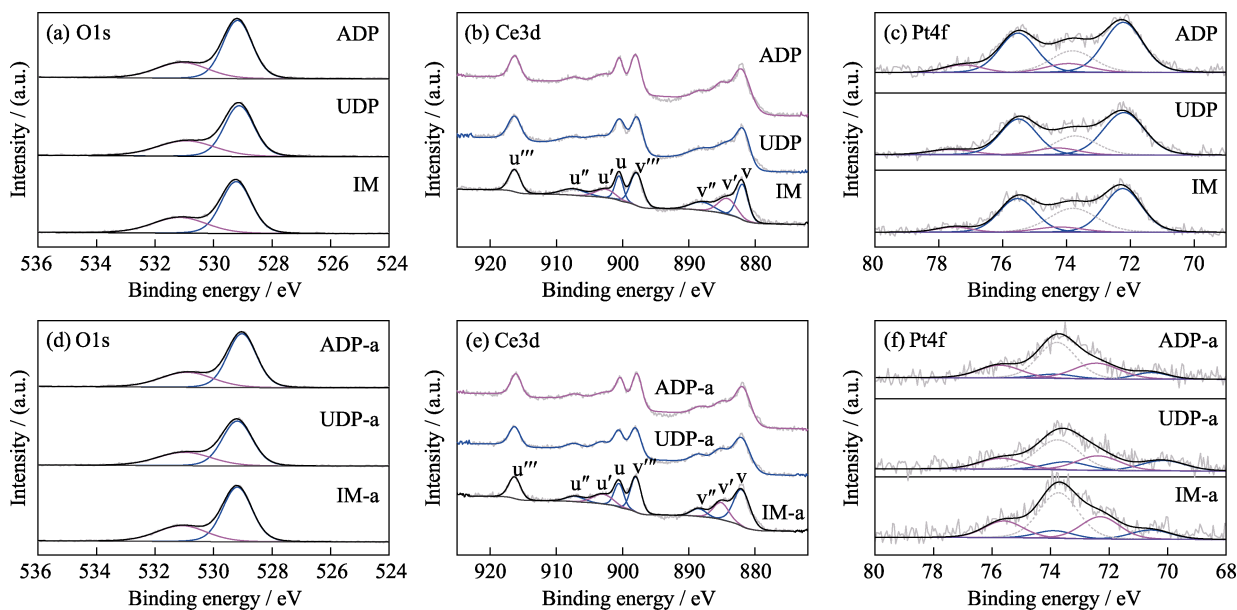

Fig. 3   XPS spectra of O1s (a, d), Ce3d (b, e) and Pt4f (c, f) for fresh (a-c) and aged (d-f) samples

As shown in Fig. 3(a, d), O_{ads} and O_{latt} exist in all samples. The ratio of O_{ads}/O for fresh samples is in the sequence of UDP > IM > ADP, but the aged samples exhibit a different sequence with an order of UDP-a > ADP-a > IM-a. It is observed slight decrease of O_{ads} for IM and UDP, but slight increase for ADP. As well known, more O_{ads} can enhance catalytic activity under vehicle exhaust atmosphere.

Ce^{3+} and Ce^{4+} coexist on the surface. The analysis of the relative ratio of Ce^{3+} reveal that conspicuous decline of the ratio of Ce^{3+}/Ce occurs after aging in case of UDP, slight decline for IM-a, while slight increase for ADP-a. The change trend is consistent with that of O_{ads}. Because the existence of Ce^{3+} has an important influence on oxygen vacancy which is conducive to adsorbing more oxygen from the gas[23]. Therefore, the oxygen vacancies in ADP are well maintained during hydrothermal aging treatment, which is favorable for keeping redox property as well as the catalytic performance.

Regarding Pt species, it is easy to detect that platinum species mainly exist in oxide state for the existence of Pt–O–Ce interaction as well[24]. It can be detected Table 2 that the value of Pt^{4+}/Pt follow the order of ADP > UDP > IM. ADP has the highest Pt^{4+}/Pt ratio which can be explained by the stronger interaction between Pt and support. The stronger interaction is conductive to maintaining Pt species at a more stable state. After aging, the surface concentration of Pt decreases to some extent. The platinum species mainly exist as Pt^{2+} and Pt^0 that PtO_2 decompose to Pt metal under oxidizing conditions at above 600 ℃[3]. What should be mentioned is that UDP-a has higher relative percent of Pt^0, which suggests that the stability of UDP-a is poor. However, ADP-a has relative higher ratio of Pt^{2+}, which also proves that ADP has a better ability to resist hydrothermal treatment.

In conclusion, from the analysis of XPS data, ADP prepared by ammonia-assisted deposition precipitation method possess stronger metal-support interaction to resist aging treatment.

2.4　H₂-TPR studies

The H₂-TPR profiles are displayed in Fig. 4. It is observed that IM has two reduction peaks. One peak at 198 ℃ is assigned to the reduction of PtO_x and Ce species that are effectively promoted by noble metal for the spillover effect[25]. The other peak at 380 ℃ is assigned to the reduction of a very low percent of surface un-activated oxygen. UDP also has two reduction peaks. The first peak at 174 ℃ is lower than that of IM, implying that UDP possess better reducibility than IM due to the better dispersion of Pt species. Attention should be paid to ADP. In the range of low temperature, ADP has a main reduction peak and two shoulder peaks with the corresponding temperature at 106, 150 and 174 ℃. Combining the analysis above, the lower reduction temperature can be ascribed to the stronger interaction in ADP. In addition, the three reduction peaks can be ascribed to the reduction of the PtO_x species and Ce species with different degree of interaction. This can be explained as a consequence of the existence of small and big particles in ADP. The reason for the smaller area of reduction peak is that the big Pt particles have a weaker promoting effect on the support.

After hydrothermal aging treatment, the reduction peaks for aged catalysts shift to higher temperature due to the sintering and agglomeration of active components. It should be noted that the temperature of the main reduction peak of UDP-a shift from 174 ℃ to 202 ℃, while that of ADP-a only shift from 150 ℃ to 164 ℃. The result suggests that the ADP undergone slighter sintering and the redox properties were well maintained, which proved the better hydrothermal stability in case of ADP.

Table 2　Surface elemental state ratio derived from by XPS

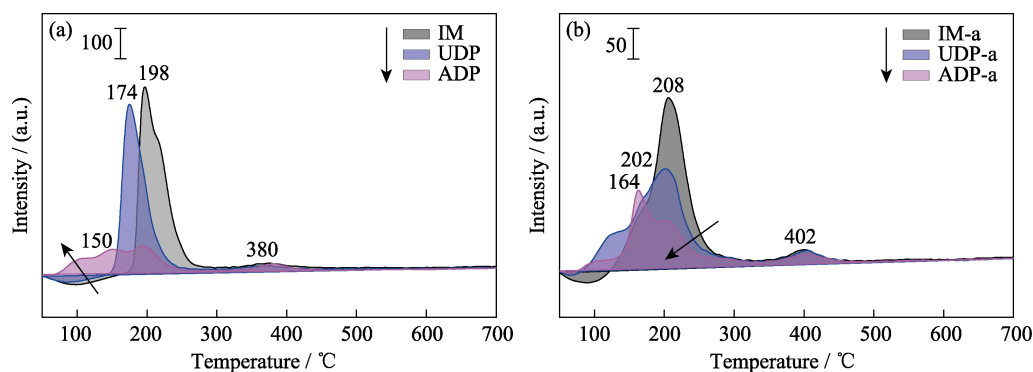| Sample	Pt^0/Pt ratio	Pt^{2+}/Pt ratio	Pt^{4+}/Pt ratio	O_{ads}/O ratio	Ce^{3+}/Ce ratio
IM	0	0.871	0.129	0.354	0.217
UDP	0	0.851	0.149	0.374	0.240
ADP	0	0.831	0.169	0.324	0.201
IM-a	0.302	0.698	0	0.329	0.195
UDP-a	0.421	0.579	0	0.350	0.187
ADP-a	0.234	0.766	0	0.336	0.214

Fig. 4　H₂-TPR profiles of the fresh (a) and aged (b) samples

2.5　Catalytic performance

The conversion curves of CO, NO, C_3H_8 and C_3H_6 for all series of samples are depicted in Fig. 5. For fresh catalysts, UDP exhibits better CO conversion activity than the reference sample IM due to the higher dispersion of Pt species and higher content of O_{ads}. ADP exhibits worse catalytic activity for all pollutions due to the worse dispersion of Pt species.

As for the aged samples, the catalytic activities are in the sequence of ADP-a>IM-a>UDP-a. The activity results exhibit converse sequence with the fresh samples. In order to compare durability carefully, the light-off temperature (T_{50}, the temperature where pollutions obtained 50% conversion), and the ΔT (defined as T_{50} of aged samples − T_{50} of fresh samples) are summarized in Table 3. ΔT is an important parameter to evaluate the stability of TWCs. The T_{50} of UDP-a shifts to higher temperature with ΔT of 87 ℃ for CO, 54 ℃ for NO, 55 ℃ for C_3H_8 and 59 ℃ for C_3H_6. This may be ascribed to that the smaller particles are easily agglomerated together, which leads to the sharp decline of dispersion of Pt species and catalytic activity. A similar situation is also found in IM-a, which T_{50} has an increase of 41, 44, 43, 44 ℃ respectively. Whereas the ΔT of T_{50} over ADP is 16 ℃ for CO, 17 ℃ for NO, 22 ℃ for C_3H_8 and 18 ℃ for C_3H_6. This indicates that ADP has better ability to maintain catalytic activity against hydrothermal treatment. ADP possess bigger Pt particles and stronger interaction in essence, which are favorable for enhancing the catalytic stability.

3　Conclusions

We have prepared Pt/CZ catalysts by two different alkali-assisted deposition precipitation method. The effects of two different alkali on the physicochemical properties, catalytic activity and durability of the catalysts were investigated.

Some important results and conclusions are presented as follows: (1) UDP showed poor aging resistance that the catalytic activity decreased seriously after hydrothermal aging treatment. (2) ADP exhibited good anti-aging ability, with little physicochemical properties and catalytic activity changed after aging. (3) The different alkali-assisted deposition precipitation methods have an important influence on the initial particle size of Pt and interaction in the catalyst, resulting in a great difference in durability.
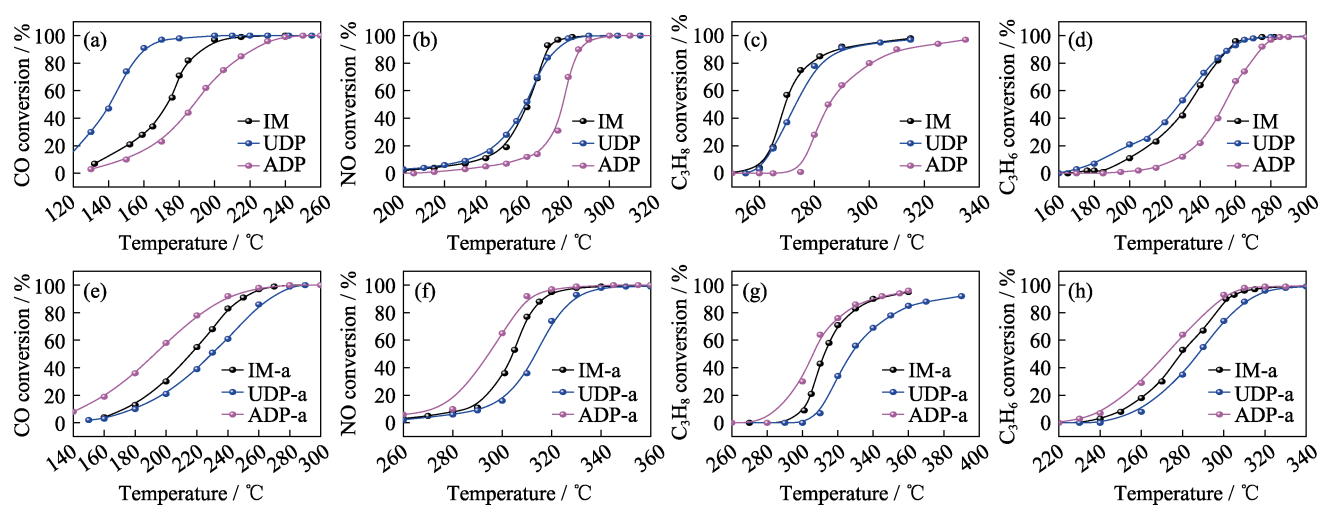

Fig. 5　Conversion curves of CO, NO, C_3H_8 and C_3H_6 over the fresh (a-d) and aged (e-h) samples, respectively

Table 3　Light-off (T_{50}) temperature and ΔT for three-way catalytic reactions over catalysts

Sample	CO		NO		C_3H_8		C_3H_6	
	T_{50}/℃	ΔT/℃	T_{50}/℃	ΔT/℃	T_{50}/℃	ΔT/℃	T_{50}/℃	ΔT/℃
IM	174	–	260	–	269	–	234	–
UDP	142	–	259	–	273	–	228	–
ADP	187	–	277	–	284	–	254	–
IM-a	215	41	304	44	312	43	278	44
UDP-a	229	87	313	54	328	55	287	59
ADP-a	203	16	294	17	306	22	272	18

References:

[1] LI G F, WANG Q Y, ZHAO B, *et al*. A new insight into the role of transition metals doping with CeO_2-ZrO_2 and its application in Pd-only three-way catalysts for automotive emission control. *Fuel*, 2012, **92:** 360–368.

[2] HANEDA M, SHINODA K, NAGANE A, *et al*. Catalytic performance of rhodium supported on ceria-zirconia mixed oxides for reduction of NO by propene. *Journal of Catalysis*, 2008, **259:** 223–231.

[3] NAGAI Y, HIRABAYASHI T, DOHMAE K, *et al*. Sintering inhibition mechanism of platinum supported on ceria-based oxide and Pt-oxide-support interaction. *Journal of Catalysis*, 2006, **242:** 103–109.

[4] ZHAN Z C, LIU X J, HE H, *et al*. Fabrication of a flower-like Pd/CeO_2 material with improved three-way catalytic performance. *Journal of Rare Earths*, 2013, **31:** 750–758.

[5] FERNANDESA D M, SCOFIELDA C F, NETO A A, *et al*. Thermal deactivation of Pt/Rh commercial automotive catalysts. *Chemical Engineering Journal*, 2010, **160:** 85–92.

[6] ESCHEMANN T O, BITTER J H, JONG K P. Effect of thermal ageing on the structure and catalytic activity of Pd/CeO_2 prepared using arc-plasma process. *Catalysis Science Technology*, 2014, **4:** 2990–2996.

[7] YOON D Y, KIM Y J, LIM J H, *et al*. Thermal stability of Pd-containing $LaAlO_3$ perovskite as a modern TWC. *Journal of Catalysis*, 2015, **330:** 71–83.

[8] TANABE T, NAGAI Y, DOHMAE K, *et al*. Sintering and redispersion behavior of Pt on Pt/MgO. *Journal of Catalysis*, 2008, **257:** 117–124.

[9] WANG J H, CHEN H, HU Z C, *et al*. A review on the Pd-based three-way catalyst. *Catalysis Reviews*, 2014, **57:** 79–144.

[10] HE J J, WANG H X, ZHENG T T, *et al*. Thermally induced deactivation and the corresponding strategies for improving durability in automotive three-way catalysts. *Johnson Matthey Technology Review*, 2016, **60:** 196–203.

[11] LI H M, LAN L, CHEN S H, *et al*. Preparation of $Ce_xZr_{1-x}O_2$ with combined composition for improved Pd-only three-way catalyst. *Journal of Inorganic Materials*, 2018, **33(7):** 798–804.

[12] WU Q F, CUI Y J, ZHANG H L, *et al*. Preparation of ceria-zirconia mixed oxides with improved thermal stability for three-way catalysts by a modified co-precipitation method. *Journal of Inorganic Materials*, 2017, **32(3):** 331–336.

[13] FAN J, CHEN Y S, JIANG X, *et al*. A simple and effective method to synthesize Pt/CeO_2 three-way catalysts with high activity and hydrothermal stability. *Journal of Environmental Chemical Engineering*, 2020, **8:** 104236–104243.

[14] MUNNIK P, JONGH P E, JONG K P. Recent developments in the synthesis of supported catalysts. *Chemical Reviews*, 2015, **115:** 6687–6718.

[15] ESCHEMANN T O, BITTER J H, JONG K P. Effects of loading and synthesis method of titania-supported cobalt catalysts for Fischer-Tropsch synthesis. *Catalysis Today*, 2014, **228:** 89–95.

[16] MOREAU F, BOND G C. Gold on titania catalysts, influence of some physicochemical parameters on the activity and stability for the oxidation of carbon monoxide. *Applied Catalysis A: General*, 2006, **302:** 110–117.

[17] PACELLA M, GARBUJO A, FABRO J, *et al*. PGM-free $CuO/LaCoO_3$ nanocomposites: new opportunities for TWC application. *Applied Catalysis B: Environmental*, 2018, **227:** 446–458.

[18] CHENG T Q, WANG J L, WANG S N, *et al*. Citric acid induced promoted dispersion of Pt on the support and enhanced catalytic activities for a Pt-based catalyst. *Applied Surface Science*, 2017, **426:** 745–754.

[19] BAZIN P, SAUR O, LAVALLEY J C, *et al*. FT-IR study of CO adsorption on Pt/CeO_2: characterisation and structural rearrangement of small Pt particles. *Physical Chemistry Chemical Physics*, 2005, **7:** 187–194.

[20] SHEN M Q, LÜ L F, WANG J Q, *et al*. Study of Pt dispersion on Ce based supports and the influence on the CO oxidation reaction. *Chemical Engineering Journal*, 2014, **255:** 40–48.

[21] FAN J, WU X D, YANG L, *et al*. The SMSI between supported platinum and CeO_2-ZrO_2-La_2O_3 mixed oxides in oxidative atmosphere. *Catalysis Today*, 2007, **126:** 303–312.

[22] PENG R S, LI S J, SUN X B, *et al*. Size effect of Pt nanoparticles on the catalytic oxidation of toluene over Pt/CeO_2 catalysts. *Applied Catalysis B: Environmental*, 2018, **220:** 462–470.

[23] FAN J, WU X D, WU X D, *et al*. Thermal ageing of Pt on low-surface-area CeO_2-ZrO_2-La_2O_3 mixed oxides: effect on the OSC performance. *Applied Catalysis B: Environmental*, 2008, **81:** 38–48.

[24] WU X D, FAN J, RAN R, *et al*. Effect of preparation methods on the structure and redox behavior of platinum-ceria-zirconia catalysts. *Chemical Engineering Journal*, 2005, **109:** 133–139.

[25] ZHANG H L, WANG J L, ZHANG Y H, *et al*. A study on H_2-TPR of $Pt/Ce_{0.27}Zr_{0.73}O_2$ and $Pt/Ce_{0.27}Zr_{0.70}La_{0.03}O_x$ for soot oxidation. *Applied Surface Science*, 2016, **377:** 48–55.

不同碱辅助的沉积沉淀法对三效催化剂稳定性的影响

范 君[1], 江 雪[2], 焦 毅[2], 陈宇圣[1], 王健礼[1], 陈耀强[1,2]

(四川大学 1. 化学学院; 2. 新能源与低碳技术研究院, 成都 610064)

摘 要: 老化处理会导致三效催化剂(TWCs)严重失活, 因此提高催化剂的耐久性能是 TWCs 设计的目标。本工作采用不同碱辅助的沉积沉淀法, 即尿素辅助沉积沉淀法和氨水辅助沉积沉淀法制备了 $Pt/Ce_{0.4}Zr_{0.5}La_{0.05}Pr_{0.05}O_2$ (Pt/CZ) 三效催化剂, 分析了不同碱对催化剂物理化学性质、催化活性和耐久性的影响。结果表明, 尿素辅助沉积沉淀法 (UDP)制备的 Pt/CZ 催化剂的抗老化性能较差, 而氨水辅助沉积沉淀法(ADP)制备的催化剂的抗老化能力较强。XRD, CO 吸附, XPS 和 H_2-TPR 表征结果表明, ADP 中较大的 Pt 颗粒以及更强的金属载体相互作用使 ADP 在老化过程中烧结程度较低, 有利于维持催化活性。因此, ADP 催化剂具有一定的工业应用前景。

关 键 词: 三效催化剂; 沉积沉淀; 碱辅助; 稳定性

中图分类号: O643   **文献标志码:** A